Improvement of PHEMT Intermodulation Prediction Through the Accurate Modelling of Low-Frequency Dispersion Effects

A.Raffo[•*], A.Santarelli[°], P.A.Traverso[°], M.Pagani[*], F.Palomba[*], F.Scappaviva[Δ], G.Vannini[•], F.Filicori[°]

[•] Department of Engineering, University of Ferrara, Via Saragat 1, 44100 Ferrara, Italy.
[°] Department of Electronics, University of Bologna, Viale Risorgimento 2, 40136 Bologna, Italy.
[*] CoRiTeL, Via Anagnina 203, 00040 Morena (Rome), Italy.
[Δ] MEC s.r.l., Viale Pepoli 3/2, 40123 Bologna, Italy.

Abstract **— Large-signal dynamic modelling of III-V FETs cannot be simply based on dc *i/v* characteristics, when accurate performance prediction is needed. In fact, dispersive phenomena due to self-heating and/or traps (surface state densities and deep level traps) must be taken into account since they cause important deviations in the dynamic drain current.**

In this paper, a recently proposed large-signal *i/v* measurement setup is exploited to extract an empirical model for low-frequency dispersive phenomena in microwave electron devices. This *i/v* model is then embedded into a microwave large-signal PHEMT model. Eventually, a Ka-band highly linear power amplifier, designed by Ericsson using the Triquint GaAs 0.25μm PHEMT process, is used for model validation.

Excellent intermodulation distortion predictions are obtained with different loads despite the extremely low power level of IMD products involved. This entitles the proposed model to be also used in the PA design process instead of conventional load-pull techniques whenever the high-linearity specifications play a major role.

Index Terms **— FETs, Semiconductor device modeling, Nonlinear circuits, Nonlinear distortion, Intermodulation distortion.**

I. INTRODUCTION

Accurate nonlinear modelling of III-V FETs for microwave circuit design should also account for low-frequency dispersive phenomena of the electrical characteristics due to deep level traps and surface state densities. Moreover, the long time constants associated with dynamic phenomena due to thermal effects are not always so much different from those associated with traps or surface states (typically from fractions to hundreds of microseconds). Consequently, dispersion due to traps cannot always be addressed separately from thermal phenomena due to power dissipation. All those phenomena cause considerable deviations between static and low frequency dynamic drain current characteristics[1], which cannot be ignored when accurate nonlinear models are needed. Many efforts have been made by several research groups to take into account low-frequency dispersion both in mathematical and equivalent circuit models.

In order to improve the prediction accuracy, some modelling approaches use pulsed *i/v* measurements, beside dc and small-signal data, for parameter identification. In fact, pulsed measurement systems allow, in theory, for a better low-frequency dispersion characterisation involving large-signal dynamic operation. In practice, besides requiring special-purpose setups, the application of narrow voltage pulses presents some drawbacks. For example, a critical point is related to the extremely wide spectrum of the pulsed-waveform. As a matter of fact, the actual accuracy achievable by pulsed measurement systems seems to be inadequate to provide very accurate models, especially when intermodulation distortion prediction capabilities at very low power levels are involved.

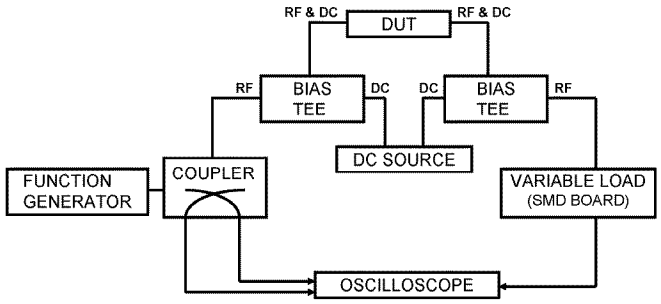

Fig. 1. The proposed large-signal measurement setup.

As an alternative to pulsed characterisation, a large signal *i/v* measuring system has been recently presented [1], where device operation is kept very similar to that involved in typical microwave circuits: large-signal sinusoidal or distorted sinusoidal regime. In fact, as can be seen in Fig. 1, the DUT is simply excited by a large-signal low frequency sinusoidal voltage source with 50 Ω internal impedance. Moreover, the device is loaded by selectable resistive impedances, while a digital sampling oscilloscope allows for the acquisition of the waveforms at the transistor ports. Full automatic remote controlling software through a standard IEEE488 interface was developed in order to "dynamically reach", with peak

[1] The *"low-frequency"* term is used here referring to the frequency range between the cutoff of dispersive phenomena and the lowest frequency where reactive effects, related to charge storage variations and finite transit times, cannot be further neglected.

0-7803-8846-1/05/$20.00 (C) 2005 IEEE

values (maximum or minimum) of the input and output device voltage waveforms, an arbitrary grid over the (v_g, v_d) domain [1].

In Section II it is shown how measurements carried out with the proposed instrumentation can be efficiently exploited for the identification of an innovative device model suitable for operation at frequencies above the cut-off of the dispersive phenomena. In Section III, the validation of the model at microwave frequencies is addressed, in conjunction with a non-quasi-static large-signal model, namely the Nonlinear Discrete Convolution (NDC) model [2-3]. Intermodulation prediction of a PHEMT-based highly linear power amplifier at Ka-band, designed and realized by Ericsson Lab Italy, is chosen as the most appropriate test case.

II. LOW-FREQUENCY I/V PHEMT MODELLING

In microwave circuit HB analysis the lowest RF spectral component to be considered is usually well above the cut-off frequencies associated with dispersive phenomena. Under such condition, any possible set of state variables $\underline{x}$ used to describe the "slow" dynamic phenomena associated with traps is practically coincident with its dc value $\underline{X_0}$. The same consideration is obviously valid for the channel temperature $\theta(t) \cong \theta_0$, which in the context of circuit-design-oriented modelling is assumed to be uniform along the channel. Thus, at frequencies above the cut-off of dispersive phenomena, but low enough to neglect microwave reactive effects due to junction charge storage or transit times, the drain current of a III\V FET can be expressed in the form:

$$i_d(t) = F(v_g(t), v_d(t), \underline{X_o}, \theta_o) \tag{1}$$

where F is a purely algebraic nonlinear function, while $v_g(t)$ and $v_d(t)$ are the instantaneous voltages applied to the device ports.

The vector $\underline{X_0}$ of the dc components of the state variables associated with the traps is here assumed as only dependent on the mean values V_{g0}, V_{d0} of the external voltages $v_g(t)$ and $v_d(t)$, as in [4]. Moreover, the junction temperature θ_0 is considered as linearly dependent on the average dissipated power under dynamic conditions P_0, i.e.,: $\theta_0 = \theta_C + R_\theta \cdot P_0$, where θ_C is the case (or substrate) temperature and R_θ is the device thermal resistance. On this basis, the following low frequency dynamic (above cut-off) drain current model is adopted here:

$$\begin{aligned} i_d(t) = {} & F^{DC}\left\{v_g(t), v_d(t), \theta_c^*\right\} + f_g\left\{v_g(t), v_d(t)\right\}\left(v_g(t) - V_{g0}\right) + \\ & + f_d\left\{v_g(t), v_d(t)\right\}\left(v_d(t) - V_{d0}\right) + f_{\vartheta_c}\left\{v_g(t), v_d(t)\right\} R_\vartheta \left(p_s(t) - P_0\right) \end{aligned} \tag{2}$$

where: F^{DC} is the static drain current characteristic at a constant reference case temperature θ_c^*, $p_s(t)$ is a "quasi-static" term corresponding to the power that would be dissipated if $v_g(t)$, $v_d(t)$ were "slowly" time-varying voltages:

$$p_s(t) = v_d(t) \cdot F^{DC}(v_g(t), v_d(t), \theta_c) \tag{3}$$

and f_g, f_d, $f_{\theta c}$ are three suitable look-up-table based parameter functions to be identified.

The dynamic drain current model (2), which can be derived[2] from (1) after linearization with respect to V_{g0}, V_{d0}, θ_0 and some algebraic manipulations, consists of the dc current component modified by means of three additive terms. These take into account the deviations between the static and the dynamic current due to traps and thermal effects. In particular, the three functions f_g, f_d $f_{\theta c}$ can be related to the $F(\cdot)$ and $F^{DC}(\cdot)$ functions by the following relationships:

$$f_g = -\left.\frac{\partial F(v_g(t), v_d(t), \underline{X_o}, \theta_o)}{\partial V_{g0}}\right|_* \tag{4}$$

$$f_d = -\left.\frac{\partial F(v_g(t), v_d(t), \underline{X_o}, \theta_o)}{\partial V_{d0}}\right|_* \tag{5}$$

$$f_{\vartheta_c} = -\left.\frac{\partial F^{DC}(v_g(t), v_d(t), \theta_c)}{\partial \theta_c}\right|_* \tag{6}$$

A new formulation of the thermal model is adopted in (2) with respect to [4]. In particular, the introduction of the "quasi static power" term $p_s(t)$ in (3) provides a model where the three dynamic additive terms become deviations of the *measured* instead of the (ideal) *equithermal* dc drain current component, as in [4].

Differentiation of (2) with respect to $v_g(t)$ and $v_d(t)$ around a generic bias condition (V_{g0} , V_{d0}) leads to:

$$\begin{aligned} & g_m^{AC}\left\{V_{g0}, V_{d0}\right\} = g_m^{DC}\left\{V_{g0}, V_{d0}\right\} + f_g\left\{V_{g0}, V_{d0}\right\} + \\ & + f_{\vartheta_c}\left\{V_{g0}, V_{d0}\right\} \cdot R_\theta \cdot g_m^{DC}\left\{V_{g0}, V_{d0}\right\} \cdot V_{d0} \end{aligned} \tag{7}$$

$$\begin{aligned} & g_d^{AC}\left\{V_{g0}, V_{d0}\right\} = g_d^{DC}\left\{V_{g0}, V_{d0}\right\} + f_d\left\{V_{g0}, V_{d0}\right\} + \\ & + f_{\vartheta_c}\left\{V_{g0}, V_{d0}\right\} \cdot R_\theta \cdot \left(g_d^{DC}\left\{V_{g0}, V_{d0}\right\} \cdot V_{d0} + I_{d0}\right) \end{aligned} \tag{8}$$

where g_m^{AC}, g_d^{AC}, g_m^{DC}, g_d^{DC} represent the trans- and output-conductance under low-frequency (ac) and static (dc) conditions, while I_{d0} is the static drain current.

For each (v_g ,v_d) pair the three model functions f_g, f_d, $f_{\theta c}$ are identified by minimizing the squared discrepancies between (2), (7), (8) and the corresponding dynamic measurements obtained under different operating conditions. In particular, large-signal low-frequency *i/v* data, obtained through the sinusoidal measurement setup [1], and small-signal low-

[2] The derivation of the dynamic current correction due to the trapping phenomena is given in [4]. Instead, the derivation of the thermal correction in (2) has not yet been published.

frequency conductances obtained from a conventional VNA are considered here. Due to the linear dependence of parameters in model equations, the identification procedure can be carried out in closed form, avoiding nonlinear numerical optimisation techniques.

III. EXPERIMENTAL RESULTS

The low-frequency model presented in Section II was identified for a 0.25 µm Triquint GaAs PHEMT (W=600µm). The latter was then embedded into a non-quasi-static large-signal device model for micro- and millimetre-wave applications, the Nonlinear Discrete Convolution (NDC) model [2,3]. To this aim, the NDC model was identified on the basis of bias- and frequency-dependent S parameters measured up to 110 GHz. A three delays model structure was used, with T_M = 1.8 ps.

In order to evaluate the nonlinear, high-frequency prediction accuracy of the model, measurements of the third-order intermodulation product (interferer) to carrier ratio (I/C) were carried out at the frequency of 39.9 GHz (two tone displacement: 10 MHz; class-A operation: I_{d0} = 60 mA, V_{d0} = 6.5V) under different loading conditions. Simulation and measurement results are shown in Fig. 2 as a function of the output power. As can be seen, the model is in very good agreement with measurements, despite the very low level of the IMD products required by the specific application. In the same figure, also the poor prediction capability obtained by using the purely static dc *i/v* characteristics instead of the low-frequency dynamic *i/v* model is shown.

The prediction accuracy of the NDC model has been tested also by means of a highly linear power amplifier designed and realized by Ericsson with the 0.25 µm Triquint GaAs PHEMT process. The amplifier, namely the Ericsson PA38, works in the 37-40 GHz frequency range and was designed for point-to-point digital radios operating with high spectral efficiency modulation schemes (up to 128 QAM). Chip size is 5.2x3.2 mm^2. In Fig. 3 the amplifier layout is shown. The PA is composed on two branches coupled by means of Lange couplers. Each branch is composed of three amplification stages; the third amplifier stage is based on the PHEMT device whose intermodulation characteristics are shown in Fig. 2. The balanced structure ensures very good input and output return losses. The output loads were chosen adopting the following strategy. The last stage output loads were set to have the minimum IMD; the 2nd stage output loads were chosen as a trade-off between linearity and gain performances. This choice resulted in a slight degradation (1 to 2 dBc) of the overall IMD performances. The first stage loads were chosen for maximizing the small signal gain.

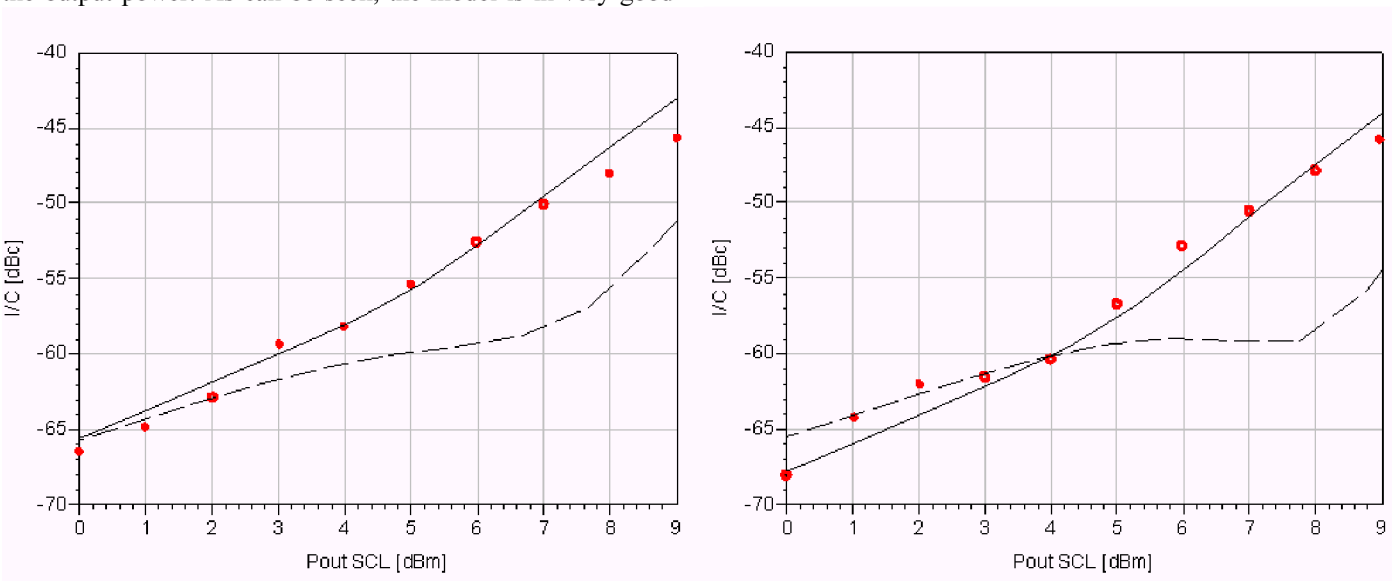

Fig. 2. Third-order intermodulation product (Interferer) to Carrier ratio versus output power (Single Carrier Level) for the 0.25µm Triquint GaAs PHEMT at 39.9 GHz [Bias: I_{d0} = 60 mA, V_{d0} = 6.5 V, Load Z_L = 10.718 + j*5.016 (left) Z_L = 8.918 + j*5.090 (right), Source Z_S = 3.45 – j*1.28]. Measurements (circles) are compared to predictions based on the NDC model [2] with embedded the new empirical model (solid line) and with the purely static dc I\V characteristic (dashed line).

Measurements carried out on the Ericsson PA38 and simulations based on the PHEMT models extracted are compared here. In particular, the I/C ratio is shown in Fig. 4 as a function of the output power, for two different bias conditions corresponding to A and AB class of operation. As can be appreciated, the simulations show an overall very good agreement with measurements confirming the high degree of prediction accuracy. In the same figure, also the poor prediction capability, due to the lack of the low-frequency dispersion modelling, obtained with the purely static I\V characteristics is shown.

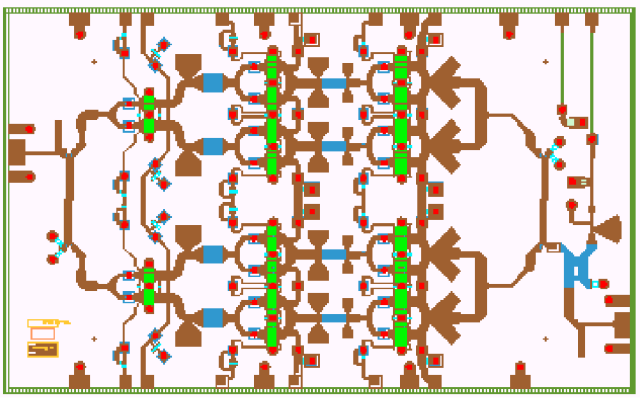

Fig. 3. Layout of the Ericsson PA38 highly-linear power amplifier

IV. Conclusion

In this paper a new *i/v* empirical model for the characterization of low-frequency dispersive effects has been presented which exploits, in the identification phase, large-signal *i/v* measurements carried out with a recently proposed measurement system [1].

The empirical model was embedded in a large-signal device model for micro- and millimetre-wave applications [2,3]. Intermodulation measurements were carried out at Ka frequencies on a single PHEMT device and on a MMIC highly linear power amplifier, demonstrating in both cases a very accurate agreement with model prediction.

Acknowledgement

This work was partly funded by the Italian Ministry of Instruction, University and Research within the project "Modelli di dispositivi elettronici per il progetto di circuiti integrati monolitici a microonde ed onde millimetriche per collegamenti radio di nuova generazione ad elevate prestazioni" and also performed in the context of the network TARGET – "Top Amplifier Research Groups in a European Team" supported by the Information Society Technologies Programme of the EU under contract IST-1-507893-NOE, www.target-net.org.

References

[1] A.Raffo, A.Santarelli, P.A.Traverso, G.Vannini, F.Filicori, "On-wafer I/V measurement setup for the characterization of low-frequency dispersion in electron devices," in *IEEE 63rd ARFTG Dig.*, Jun. 2004, pp. 21 – 28.

[2] F.Filicori, A.Santarelli, P.A.Traverso, G.Vannini, "Electron Device Model Based On Nonlinear Discrete Convolution For Large-Signal Circuit Analysis Using Commercial Cad Packages," in *Proc. of GAAS*, Oct. 1999, pp. 225 – 230.

[3] A.Costantini, R.P.Paganelli, P.A.Traverso, G.Favre, D.Argento, M.Pagani, A.Santarelli, G.Vannini, F.Filicori, "Accurate prediction of PHEMT intermodulation distortion using the nonlinear discrete convolution model," in *2002 IEEE MTT-S Int. Microwave Symp. Dig.,* vol.2, pp.857 – 860.

[4] F.Filicori, G.Vannini, A.Santarelli, A.M.Sanchez, A.Tazon and Y.Newport, "Empirical modeling of low-frequency dispersive effects due to traps and thermal phenomena in III-V FET's," *IEEE Trans. MTT,* vol. 43, pp. 2972-2981, Dec. 1995.

[5] F.Palomba, M.Pagani, I. De Francesco, A.Meazza, G. Sivverini et al. "Process-tolerant High-Linearity MMIC Power Amplifiers," in *Proc. of GAAS*, Oct. 2003, pp. 73-76.

[6] K.Lu P.McIntosh, C.M.Snowden, R.D.Pollard, "Low-Frequency dispersion and its influence on the Intermodulation performance of AlGaAs/GaAs HBTs," in *1996 IEEE MTT-S Int. Microwave Symp. Dig.*, vol. 3, pp.1373 - 1376.

[7] M.A.Smith, T.S.Howard, K.J.Anderson, A.M.Pavio, "RF Nonlinear Device Characterization Yields Improved Modeling Accuracy," in *1986 IEEE MTT-S Int. Microwave Symp. Dig.*, vol. 86, pp.381 - 384.

[8] J.Rodriguez-Tellez, T.Fernandez, A.Mediavilla and A.Tazon, "Characterization of Thermal and Frequency-Dispersion Effects in GaAs MESFET Devices," *IEEE Trans. MTT,* vol.49, No. 7, pp. 1352 – 1355, Jul. 2001.

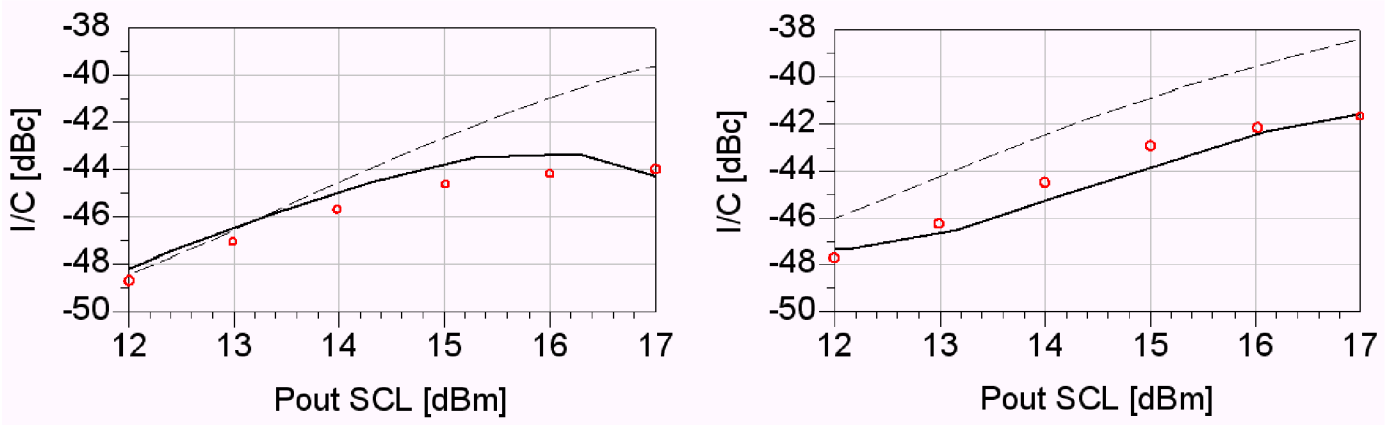

Fig. 4. Interferer to Carrier ratio versus output power (Single Carrier Level) for the highly-linear power amplifier Ericsson PA38 at 38 GHz [Bias for the last stage: I_{d0} = 600 mA (left), I_{d0} = 450 mA (right)]. Measurements (circles) are compared to predictions based on the NDC model [2] with embedded the new empirical model (solid line) and with the purely static dc i\v characteristic (dashed line).